2005 International Linear Collider Workshop - Stanford, U.S.A.

Higgs parity measurement at the ILC

Andreas Imhof
DESY, Notkestrasse 85, 22607 Hamburg, Germany and
Universität Hamburg, Institut für Experimentalphysik Luruper Chaussee 147, 22761 Hamburg, Germany

The prospects for a measurement of the Higgs parity in the $h\tau\tau$ coupling are discussed for a Higgs boson of 120 GeV mass, produced in e^+e^- collisions at $\sqrt{s} = 350$ GeV. Specific angular distributions in the $H^0/A^0 \to \tau^+\tau^-$, $\tau^\pm \to \rho^\pm\bar{\nu}_\tau(\nu_\tau), \rho^\pm \to \pi^\pm\pi^0$ and $\tau^\pm \to a_1^\pm\bar{\nu}_\tau(\nu_\tau), a_1^\pm \to \pi^\pm\pi^+\pi^-$ decay chains are used to distinguish between a $\mathcal{CP}$-even and a $\mathcal{CP}$-odd Higgs boson. The study includes expected background processes and performance of a detector at the International Linear Collider (ILC), using the parameters from the TESLA TDR [1]. As an example, the production mechanism via the Standard Model Higgs-strahlung process is used. The study shows a good potential for precise reconstruction of the hadronic τ decays and a clear differentiation potential between a $\mathcal{CP}$-even H^0 and a $\mathcal{CP}$-odd A^0 Higgs boson for the given assumptions.

1. Introduction

One of the important goals in the scientific program of the ILC is to precisely measure the properties of the Higgs boson, among them its $\mathcal{CP}$ quantum numbers. This might allow for the distinction between different models, (Standard Model (SM), Minimal Supersymmetric Standard Model, general Two Higgs Doublet Models etc.) predicting different Higgs bosons. For a light Higgs boson (m_{H^0/A^0}=120 GeV), decays into $\tau^+\tau^-$ can allow the determination of the parity, as has already been shown in a theoretical study [2], using the decays $\tau^\pm \to \rho^\pm\bar{\nu}_\tau(\nu_\tau)$ with the subsequent decay $\rho^\pm \to \pi^\pm\pi^0$. In addition the decay chain $\tau^\pm \to a_1^\pm\bar{\nu}_\tau(\nu_\tau), a_1^\pm \to \rho^0\pi^\pm$ with $\rho^0 \to \pi^+\pi^-$ is used to increase the number of signal events. To enable a study which includes the full spin-effects for τ leptons originating from spin zero particles, an extension for the interface of `TAUOLA` [3–5] was developed [6]. The distinction between $\mathcal{CP}$-even and $\mathcal{CP}$-odd eigenstates of the Higgs boson can be extracted from angular distributions, constructed from the momenta of the τ decay products. The method of $\mathcal{CP}$ reconstruction does not depend on the Higgs production mechanism. For this study, the Higgs-strahlung process, $e^+e^- \to H^0Z^0$, is used as an example source for Higgs bosons.

2. The $\mathcal{CP}$ sensitive observable

The $\mathcal{CP}$ sensitive observable used in this study relies on the 4-momenta of the pions in the final state for the decays $H^0/A^0 \to \tau^+\tau^- \to \rho^+\bar{\nu}_\tau\rho^-\nu_\tau/a_1^+\bar{\nu}_\tau a_1^-\nu_\tau/a_1^\pm\nu_\tau\rho^\mp\nu_\tau$. For the case $\tau^+\tau^- \to \rho^+\bar{\nu}_\tau\rho^-\nu_\tau$, in the rest frame of the $\rho^+\rho^-$ system, the acoplanarity angle φ^* is defined as the angle between the two planes spanned by the immediate decay products (the $\pi^\pm$ and π^0) of the two $\rho^\pm$. Fig. 1 shows a sketch of this geometric correlation. As the two angles φ^* and (180°-φ^*) can be measured between the two planes, an additional criteria is needed for a non-ambiguous determination. The sign of the product $y_+ \cdot y_-$ is taken to resolve the ambiguity by using φ^* as the acoplanarity angle for the case of $y_+ \cdot y_- > 0$ and (180°-φ^*) for the case of $y_+ \cdot y_- < 0$. y_+ and y_- are defined as follows, with $E_{\pi^\pm}$ and E_{π^0} representing the reconstructed $\pi^\pm$ and π^0 energies in the laboratory frame:

$$y_\pm = \frac{E_{\pi^\pm} - E_{\pi^0}}{E_{\pi^\pm} + E_{\pi^0}}. \tag{1}$$

For the case that one or both $\tau^\pm$ decays via the $a_1^\pm$ resonance, an ambiguity has to be resolved, as two combinations of the three charged pions in the final state can originate from the intermediate ρ^0. Here the combination of $\pi^+\pi^-$ with an invariant mass closest to the ρ^0 mass is taken to span the decay plane as in the case before. As visible parts

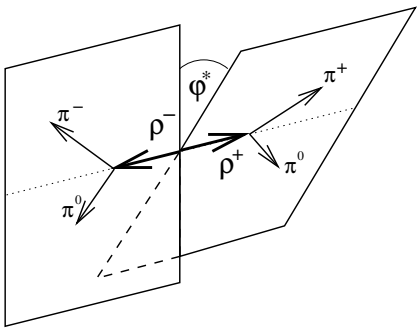

Figure 1: Acoplanarity angle φ^* between the decay planes. Each plane is spanned by the momenta of the pions from one $\tau^\pm$ decay. Shown here for the case that both $\tau^\pm$ decay via the $\rho^\pm$ resonance into $\pi^\pm\pi^0\bar{\nu}_\tau(\nu_\tau)$ in their common $\rho^+\rho^-$ rest frame.

of the final state are thus not taken into account, a reduced sensitivity is expected. For the calculation of the $y_\pm$ parameter Eq. 1 is modified, as shown here for the a_1^-case:

$$y_- = \frac{E_{\pi^+} - E_{\pi^-}}{E_{\pi^+} + E_{\pi^-}}. \tag{2}$$

The φ^* distribution is expected to be asymmetric, with the sign of the asymmetry being opposite for a scalar or a pseudo-scalar Higgs boson [2].

3. Monte Carlo simulation

Signal (Tab. I) and background events (Tab. II) are simulated for a luminosity of 1 ab^{-1} at $\sqrt{s} = 350$ GeV for a Higgs boson mass of 120 GeV. As two photon processes with $\sqrt{s^*} \geq 20$ GeV are fully rejected by the selection (chapter 5), two photon processes with 10 GeV $\leq \sqrt{s^*} < 20$ GeV have been simulated with a fraction of the luminosity only (10% for $\gamma\gamma \to \ell^+\ell^-$, 23% for $\gamma\gamma \to \mathrm{q\bar{q}}$). The events are generated with `PYTHIA 6.2` [7], taking initial state radiation into account. All $\tau^\pm$ are being decayed by `TAUOLA`, using `PHOTOS` [8] for final state radiation (FSR). FSR for all other particles is calculated by `PYTHIA`. The simulation of the spin-correlated decay is only available for $\mathrm{H^0/A^0} \to \tau^+\tau^-$. The full $\gamma^*/\mathrm{Z^0}$ interference is taken into account.

Table I: Overview on the possible final state combinations for signal events from Higgs-strahlung and their expected cross sections in ab.

$\mathrm{H^0/A^0} \to$	$\mathrm{Z^0} \to \nu\nu$	$\mathrm{Z^0} \to \mathrm{e^+e^-}/\mu^+\mu^-$	$\mathrm{Z^0} \to \mathrm{q\bar{q}}$
$\rho^+\rho^-$	166	56	582
$a_1^\pm\rho^\mp$	131	44	458
$a_1^+a_1^-$	26	9	90

Table II: Overview on the background processes taken into account and the expected cross sections.

$\mathrm{e^+e^-} \to$	final state	cross section in ab
$\gamma^*/\mathrm{Z^0}\ \gamma^*/\mathrm{Z^0}$	$\ell^+\ell^-\ \ell^+\ell^-$	$0.7 \cdot 10^5$
	$\mathrm{q\bar{q}q\bar{q}}$	$4.8 \cdot 10^5$
	$\ell^+\ell^-\mathrm{q\bar{q}}$	$4.4 \cdot 10^5$
$\mathrm{W^+\ W^-}$	$\ell^+\nu\ \ell^-\nu$	$1.4 \cdot 10^6$
	$\mathrm{q\bar{q}}\ \ell^\pm\nu$	$5.9 \cdot 10^6$
	$\mathrm{q\bar{q}q\bar{q}}$	$6.1 \cdot 10^6$
$\gamma^*/\mathrm{Z^0}$	visible	$35.0 \cdot 10^6$
$\mathrm{e_i}\gamma \to \mathrm{e_i} + \gamma^*/\mathrm{Z^0}$	$\mathrm{q\bar{q}}$	$13.3 \cdot 10^6$
	$\ell^+\ell^-$ (visible)	$5.7 \cdot 10^6$
$\mathrm{e_i}\gamma \to \mathrm{f_j} + \mathrm{W^\pm}$	$\mathrm{q\bar{q}}$	$2.5 \cdot 10^6$
	$\ell^\pm\nu$	$1.2 \cdot 10^6$
$\mathrm{H^0/A^0} + \gamma^*/\mathrm{Z^0} \to X$	not signal	$1.4 \cdot 10^5$
$\gamma\gamma(\sqrt{s^*} \geq 20GeV)$	visible	$213.3 \cdot 10^6$

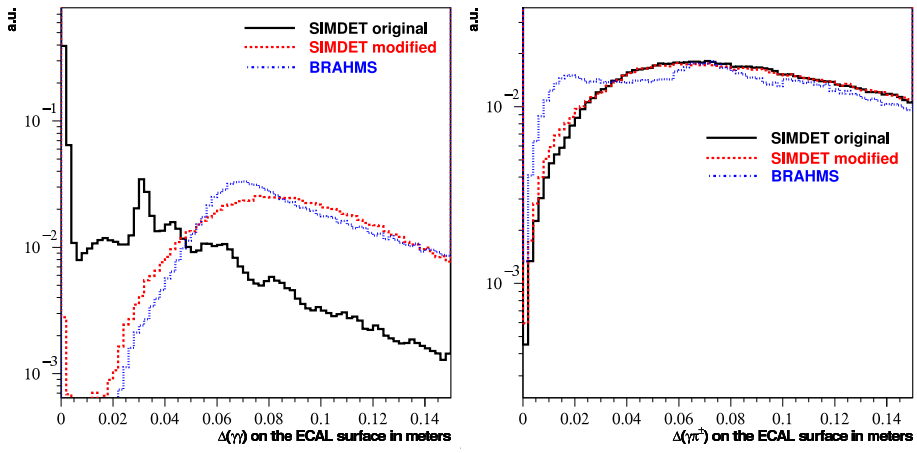

Figure 2: Distance between two reconstructed particles measured at the surface of the calorimeter, facing the tracking system. A comparison between SIMDET, BRAHMS and the enhanced version of SIMDET is given for two reconstructed photons (left), as well as for a reconstructed $\pi^{\pm}$ and up to two nearby reconstructed photons (right). If more than two photons appear close to a $\pi^{\pm}$, only the two highest energetic ones are taken into account. One of the signal channels ($e^+e^- \to H^0Z^0$, $Z^0 \to \nu\nu$, $H^0 \to \tau^+\tau^-$, $\tau^{\pm} \to \pi^{\pm}\pi^0\bar{\nu}_\tau(\nu_\tau)$ is used for this study.

4. Detector simulation

The parametrised detector simulation SIMDET [9], based on the TESLA design, is used to account for the expected performance of a detector at the ILC. This package includes also the reconstruction into particle flow objects. As this measurement relies on the exclusive reconstruction of the 4-momenta of the π^0, a realistic simulation of the calorimeter response to the $\pi^0 \to \gamma\gamma$ decays is crucial. In contrast to inclusive studies, for this measurement differences between SIMDET and the GEANT3-based [10] simulation and reconstruction tool BRAHMS [11] appear. Thus $\tau^{\pm} \to \rho^{\pm}\nu$ decays were studied with BRAHMS, to investigate the achievable energy and momentum resolution of photons, as well as the potential for a separate reconstruction in the vicinity of other particles. Fig. 2 shows the distance between two separately reconstructed photons (left) and the distance between a photon and a reconstructed $\pi^{\pm}$ (right). The too high separability of two nearby photons together with artifacts originating from the calorimeter granularity implemented in SIMDET result in significant deviations in the distribution obtained from BRAHMS and SIMDET.
The more detailed detector simulation of BRAHMS is used to build a post-processor for the calorimeter simulation of SIMDET, re-smearing the reconstructed photon energy and momentum and evaluating the influence of other reconstructed objects closer than 15 cm (neutral objects) and closer than 11.5 cm (charged objects) for all possible pairings. Below these thresholds, merging of two objects is done, according to distance dependant probabilities gained from BRAHMS. In case a charged and a neutral object are merged, the resulting calorimeter energy of the combined object is compared to the energy of the charged particle, measured in the tracking system. If the energy of the combined object significantly exceeds the energy from the tracking system, a neutral object in addition to the charged particle is reconstructed. As can be seen in Fig. 2, the application of this algorithm shows a better consistency with BRAHMS, especially for the problematic left distribution, and thus is used further on.

5. Event selection and signal identification

5.1. τ identification

To search for lepton candidates (e, μ, τ) a cone jet finding (opening angle 9.5°, minimum energy of the charged cone seed 0.7 GeV, cone energy sum at least 5 GeV) is performed [12]. Cones are accepted as lepton candidates, if they contain one or three tracks, have an invariant mass below 3 GeV, an isolation between the cone axis and the closest

other charged object above 12.5° and an angle to the beam axis of at least 9.5°. Within this candidates, electrons and muons are identified, using their typical signatures in the tracking and calorimeter systems. All remaining candidates are considered to originate from $\tau^{\pm}$.

5.2. Preselection

An event has to have a visible mass $m_{\rm vis}^{\rm evt}$ of 21 GeV $< m_{\rm vis}^{\rm evt} <$ 355 GeV and a multiplicity below 81 particle flow objects. In addition it also has to be well inside the detector with $|cos(\theta_{\rm evt})| \leq 0.995$ ($\theta_{\rm evt}$ is the angle between the direction of summed momentum of all particle flow objects and the beam axis). An event has to contain at least two hadronic τ candidates with opposite charge. At least one $\tau^+\tau^-$ combination (pair) has to have an angle α between the τ candidates of $75° < \alpha < 175°$ and an invariant mass between 21 GeV and 120 GeV. Applying these criteria results in a signal efficiency of 85%.

5.3. Separation from Standard Model backgrounds

The selection is done separately for the different decay channels of the Z^0 boson (Tab. I). For a sufficient separation of signal events originating from the Higgs-strahlung process with $H^0/A^0 \rightarrow \tau^+\tau^-$ from the background events, the reconstruction of both the Higgs and the Z^0 boson is mandatory. This discards signal events with $Z^0 \rightarrow \nu\nu$.

Signals with $Z^0 \rightarrow q\bar{q}$

The selection is based on the following four steps:

- **Global event shape:** At least 16 particle flow objects, none of them being $e^{\pm}$ or $\mu^{\pm}$, are required. The visible energy and mass must fulfill 120 GeV $< E_{\rm vis}^{\rm evt} <$ 345 GeV and 110 GeV $< m_{\rm vis}^{\rm evt} <$ 360 GeV. In addition $m_{\rm vis}^{\rm evt}$ is required to be above $(0.511 \cdot E_{\rm vis}^{\rm evt} + 48.68)$ GeV for $E_{\rm vis}^{\rm evt} \leq 208$ GeV and above $(1.217 \cdot E_{\rm vis}^{\rm evt} - 54.22)$ GeV for $E_{\rm vis}^{\rm evt} > 208$ GeV. The thrust value is required to be between 0.2 and 0.9, $|cos(\theta_{\rm thrust})| < 0.96$.

- **τ candidates:** An isolation between the candidate and the closest other charged particle between 31.8° and 134° is required. The angle between the two τ leptons has to be between 80° and 150°. For a 1-prong τ the invariant τ mass has to be between 0.40 GeV and 1.25 GeV, for a 3-prong candidate between 0.74 GeV and 1.60 GeV respectively.

- **$Z^0 \rightarrow q\bar{q}$:** The sum of the 4-momenta of all particles beside the τ pair $(E_{\rm sum}, p_{\rm sum})$ is calculated. 80 GeV $< E_{\rm sum} <$ 240 GeV and $|cos(\theta_{p_{\rm sum}})| \leq 0.95$ is required, with θ being the angle between the $p_{\rm sum}$ vector and the beam axis. A jet finding is performed, forcing all particles beside the τ pair into two jets. Events with $-1.8 < y_{12} < -0.1$ are accepted.

- **Kinematic fit:** A kinematic fit is performed, using the 4-momenta of the hadronic jets from the jet finding above and the 3-momenta of the visible τ decay products as directions for the τ jets as inputs. As constraints, the Z^0 mass and energy and momentum conservation are requested. Events with a fit result of $\chi^2 < 25$ are accepted. The recoil mass of the two hadronic jets from this fit has to satisfy 116 GeV $\leq m_{\rm recoil} \leq$ 132 GeV.

This selection results in a signal-efficiency of $\epsilon \sim 38\%$ at a signal to background ratio of 3.05 for the $\rho\rho$ channel and 1.15 for the $a_1\rho$ channel. The cut-flow is summarised in Tab. III for these two signal combinations and the most important background processes. As the a_1a_1 channel is overwhelmed by backgrounds, it is not taken into account for the measurement.

Table III: Cut-flow for the $\tau\tau$ $q\bar{q}$ selection for $\rho^+\rho^-$ and $\rho^\pm a_1^\mp$ signal and the most relevant backgrounds.

	signal	other H^0Z^0 /A^0Z^0	$Z^0Z^0 \to \tau\tau q\bar{q}$	$Z^0Z^0 \to q\bar{q}q\bar{q}$	$WW \to q\bar{q}\tau\nu$	$WW \to q\bar{q}q\bar{q}$
$N_{evt}/1ab^{-1}$	1040	140000	65270	477000	1952000	6081000
preselection	881	4849	14293	8554	198021	142905
event shape	810	2928	7961	4374	52493	57456
τ candidates	604	481	2190	7	1980	130
$Z^0 \to q\bar{q}$	594	467	1942	1	901	30
kinematic fit	410	187	97	-	6	-
$\rho\rho$ and $a_1\rho$	401	126	97	-	4	-

Signals with $Z^0 \to \ell^+\ell^-$

The selection is based on the following steps:

- **Event shape:** Between 4 and 12 particle flow objects are required, $|cos(\theta_{\text{thrust}})| < 0.96$ and $|cos(\theta_{\text{evt}})| < 0.96$.
- **$Z^0 \to \ell^+\ell^-$:** Exactly one pair of e^+e^- or $\mu^+\mu^-$ with a maximum angle of 120° between the two leptons, 82 GeV $\leq m_{\text{inv}}^{\ell^+\ell^-} \leq$ 99 GeV and 118 GeV $\leq m_{\text{recoil}}^{\ell^+\ell^-} \leq$ 160 GeV is requested. The summed $\ell^+\ell^-$ momentum ($p_{\text{sum}}^{\ell^+\ell^-}$) has to fulfill $cos(\theta_{p_{\text{sum}}^{\ell^+\ell^-}}) \leq 0.88$.
- **$\tau^+\tau^-$:** The τ candidate pair has to have an angle of between 80° and 150° between the two τ leptons. The invariant candidate masses must be 0.20 GeV $< m_{\text{invariant}}^{1-\text{prong}} <$ 1.50 GeV and 0.70 GeV $< m_{\text{invariant}}^{3-\text{prong}} <$ 1.55 GeV.

This selection results in a signal-efficiency of $\epsilon \sim 47\%$ at a signal to background ratio of 1.55 for the $\rho\rho$ channel and 0.6 for the $a_1\rho$ channel with only other H^0Z^0/ A^0Z^0 and Z^0Z^0-backgrounds remaining. As above, the a_1a_1 channel is overwhelmed by backgrounds and thus not taken into account for the measurement.

6. Measurement of the acoplanarity

The acoplanarity angles φ^* can be calculated for the remaining events and the asymmetry of the resulting acoplanarity distributions can be evaluated. The asymmetry is defined as:

$$A_{H^0/A^0} = \frac{N_{\varphi^*<\pi/2} - N_{\varphi^*>\pi/2}}{N_{\varphi^*<\pi/2} + N_{\varphi^*>\pi/2}}. \quad (3)$$

For the most important signal channel ($\rho\rho q\bar{q}$ final state) the two distributions for the acoplanarity angle φ^* for a $\mathcal{CP}$-even H^0 and a $\mathcal{CP}$-odd A^0 are shown in Fig. 3. The corresponding asymmetries are: $A_{H^0} = 0.116 \pm 0.058$ and $A_{A^0} = -0.132 \pm 0.058$ (with statistical errors only), with a resulting difference of $\Delta A = 0.248$.
This result can be interpreted as an exclusion to misidentify a measurement of a $\mathcal{CP}$-even H^0 as $\mathcal{CP}$-odd A^0 in this channel of more than 4σ. In combination with the other less sensitive final states, an overall exclusion of a misidentification of 4.7σ can be obtained with the described assumptions.

7. Conclusion and outlook

The detector at the ILC as proposed for TESLA will be able to reconstruct hadronic τ decays with high efficiency and precision. The proposed observable allows a clear distinction with 4.7σ between a $\mathcal{CP}$-even H^0 and a $\mathcal{CP}$-odd A^0 for the assumed cross sections. The detector performance has been taken into account on a higher level of detail compared to earlier studies. Higgs-strahlung with $Z^0 \to \nu\nu$ decays could not be successfully used for this analysis. Although the observable is independent of the production process, the application of this observable to e.g. a weak boson fusion channel could be problematic.

The significance might still be improved by using neural networks techniques for the signal identification or by constructing an observable with higher sensitivity.

With modifications as shown in an earlier study [13], the observable could also be used to measure a mixing angle between the $\mathcal{CP}$ phases, if the mass eigenstate is not equivalent with the $\mathcal{CP}$ eigenstate. It has to be checked, if those results can be validated with the currently achieved level of detail (detector performance and backgrounds).

Recent efforts [14] to measure a $\mathcal{CP}$ violating phase in hadronic τ decays from the Higgs, so far including only expected detector resolutions, but no realistic detector simulation and no selection from background events, show promising results.

Acknowledgments

The author wishes to thank K. Desch and T. Kraemer for the guidance in preparing this study and T. Pierzchała, M. Worek and Z. Wąs for developing the observable, enabling this study and helpful information and discussions.

References

[1] T. Behnke, S. Bertolucci, R. D. Heuer, and R. Settles, DESY-01-011.
[2] G. R. Bower, T. Pierzchała, Z. Wąs, and M. Worek, *Phys. Lett.* **B543** (2002) 227, hep-ph/0204292.
[3] S. Jadach, J. H. Kühn, and Z. Wąs, *Comput. Phys. Commun.* **64** (1990) 275.
[4] M. Jeżabek, Z. Wąs, S. Jadach, and J. H. Kühn, *Comput. Phys. Commun.* **70** (1992) 69.
[5] S. Jadach, Z. Wąs, R. Decker, and J. H. Kühn, *Comput. Phys. Commun.* **76** (1993) 361.
[6] Z. Wąs and M. Worek, *Acta Phys. Polon.* **B33** (2002) 1875, hep-ph/0202007.
[7] T. Sjöstrand *et al.*, *Comput. Phys. Commun.* **135** (2001) 238, hep-ph/0010017.
[8] E. Barberio and Z. Wąs, *Comput. Phys. Commun.* **79** (1994) 291.
[9] M. Pohl and H. J. Schreiber, hep-ex/0206009.
[10] GEANT:Cern Program Library Long Writeups W5013 (1993).
[11] T. Behnke et al., *LC-TOOL-2001-005* (2001).
[12] B. Sobloher, PhD Thesis in preparation.
[13] K. Desch, A. Imhof, Z. Was, M. Worek, *Phys. Lett.* **B579** (2004) 157, hep-ph/0307331.
[14] A. Rougé, hep-ex/0505014.

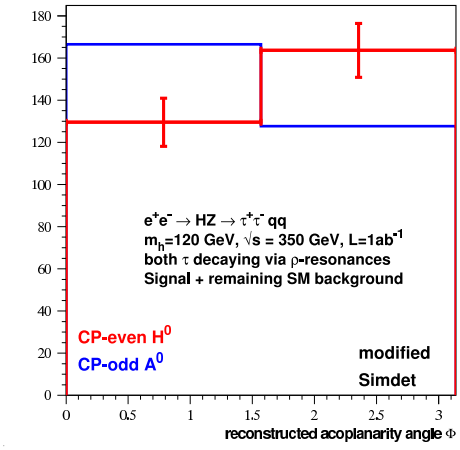

Figure 3: Distributions for the acoplanarity angle φ^* for signal and remaining background from the search for $\rho\rho q\bar{q}$ final states for 1 ab^{-1}. Both signal and the most critical background processes are scaled from a higher number of events. The thick (red) line represent the result for a $\mathcal{CP}$-even H^0 (with the statistical error per bin added), the thin line (blue) for a $\mathcal{CP}$-odd A^0.